# GAS TURBINE BLADE NATURAL FREQUENCY MEASUREMENT USING EXTERNAL CASING VIBRATIONS

Johannes Ratz[1,2], Gareth L. Forbes[1]
[1] Department of Mechanical Engineering, Curtin University
Bentley
Perth, Australia
[2] Technical University Darmstadt,
Germany
Telephone: +61 (08) 9266 3010
Gareth.Forbes@curtin.edu.au


Robert B. Randall
School of Mechanical and Manufacturing Engineering, University of New South Wales
Kensington
Sydney, Australia

**Key words**: Blade vibration; gas turbines; casing vibration; internal pressure.

**Abstract**: Currently tip timing methods are the pseudo industry standard for measuring Gas Turbine blade vibration. The physical placement of tip timing probes is however reasonably prohibitive due to the high pressure/temperature environment of a turbine. A simpler method of sensor setup would be through the use of externally mounted accelerometers to measure the casing vibration response and relate this back to the internal blade vibration.
The vibration of a gas turbine casing is driven by the strong rotating pressure which develops around the rotating blade stages. The oscillating motion of the rotor blades phase modulates this pressure signal. An analytical formulation of the internal pressure signal is developed in this paper. The effects of blade motion on this internal pressure signal is then investigated as the speed of the engine is increased/decreased such that the driving frequency traverses a rotor blade natural frequency. Experimental measurements on a simplified test turbine are presented comparing the results of the analytical internal pressure signal along with results of the measured casing vibration during engine run up/down. It is shown that the spectrum of the internal pressure and casing vibration signal contains information which can be used to estimate the rotor blade natural frequencies.

**Introduction**:  Rotor blade vibration within a gas turbine is developed by the periodic passing of the rotor blades through an unsteady pressure field. This unsteady pressure field is developed by the upstream stator blades and/or inlet guide vanes. This passing of rotor blades through high/low pressure fields is unavoidable and is indeed integral to the

operation of the engine. The need to accommodate the dynamic response of rotor blades under these oscillating forces is therefore required in the operation of these engines. The analysis and measurement of this dynamic motion is therefore required for this end. Additionally the measurement of rotor blade natural frequencies during the engine operation could have the potential to be used a parameter for condition monitoring, and provide an estimate of the development of any rotor blade faults. It should be noted that this however has not been shown to viable in the monitoring of turbine engines to date.

Rotor blade tip timing methods are the most widely used method to measure turbine blade vibration. Blade tip timing (BTT) methods measure the arrival time of rotor blades as they pass a sensor which is located around the periphery of the engine. The difference in the blade arrival time due to its oscillation around its equilibrium position, and the arrival time the blade would have if no vibration was present, allows the estimation of the blade vibration.

BTT methods can be used to measure blade vibration amplitude at a single speed with a number of sensors (>4 for synchronous response and >2 for asynchronous response) located around the engine stage. The blade natural frequency may also be measured with (1) sensor as the engine is swept across a range of speeds [1, 2].

The fundamental limitation on BTT methods, which has caused the need for significant engineering effort to attempt to over-come, is the under sampling of the blade vibration signal. The number of samples of blade vibration per rotation is only as high as the number of sensors located around the engine stage.

Previously the use of turbine casing vibration measurements as a method of measuring rotor blade vibration has been proposed, with an analytical model first developed in Ref [3]. More recently the use of the stochastic portion of the casing vibration signal has been shown to contain information which can be used to determine the natural frequency of a turbine blade at a single operating speed [4]. The inclusion of rotor blade vibration parameters in the turbine casing vibration signal develops from the influence the blade vibration has on the turbine internal pressure signal which drives the casing vibration. The oscillation of the rotor blades causes the phase modulation of the internal pressure signal. This phase modulation amplitude changes in magnitude as the rotor blade driving frequency, stator passing frequency, changes as the engine speed increases/decreases. The use of the simple measurement of the external casing vibration of a turbine and measuring parameters of the rotor blade vibration thus has benefits of measurement ease over the use of BTT methods. The development of the driving internal pressure signal including rotor blade vibration will be developed analytically in the following sections.

**Formulation of internal pressure**: The internal pressure signal inside a turbine, is created by the flow of air over the rotor and stator blade aerofoils and creates a high and low pressure field over each of these blades. This internal pressure signal is harmonic with the number of rotor blades, and is shown in a simplified schematic in Figure 1. This simplified schematic shows 6 rotor blades with the first harmonic of the internal pressure signal also shown.
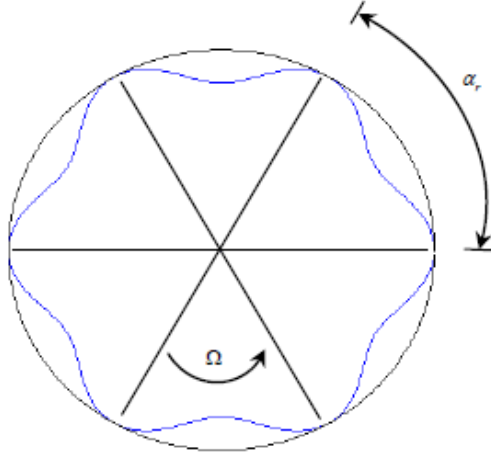
Figure 1. Schematic of simple first harmonic pressure distribution for a 6 bladed arrangement.

Consider at first the effect this internal pressure would create as the turbine rotates, without any rotor blade vibration, then the internal pressure signal can be expressed mathematically as Fourier series expansion as given in equation (1) for the 'r[th]' rotor blade.

$$P_r = \text{Re}\left\{ \sum_{i=0}^{\infty} A_i P e^{ji[\theta + \Omega t + \alpha_r + \gamma_i]} \right\} \tag{1}$$

In equation (1) P is the magnitude of the pressure, $A_i$ and $\gamma_i$ are the amplitude and the phase of the Fourier series, $\theta$ is the angular position around the casing for any given datum, $\Omega$ is the shaft speed and $\alpha_r$ the angle between two adjacent blades.

When the pressure signal is summed for all rotor blades, then the internal pressure will cause a fluctuating pressure on the internal surface of the turbine casing at multiple frequencies of the rotor blade passing frequency. This will therefore cause the largest component of casing vibration to be driven at these multiples of rotor blade passing frequency, which has been shown to be found in experimental measurements [5].

**Influence of blade vibration**: As the rotor blades oscillate about their equilibrium position, the influence this has in the internal pressure signal will now be developed. As mentioned previously, the dominant excitation frequency of the rotor blade vibration, is the traversing of the high and low pressure fields from the upstream stator rows, this causes a dominant excitation force on the rotor blade at multiples of stator passing frequency. The rotor blades are modeled in this study as a single degree of freedom lumped spring-mass system, hence the displacement of the rotor blades is given by equation (2)-(3) wherein $\omega_{spf}$ is the stator passing frequency, $\gamma_r$ the phase offset for the force of each blade and B the amplitude defined by equation (3).

$$x(t)_r = B \sin\left( \omega_{spf} t + \gamma_r \right) \tag{2}$$

$$B = \frac{F_0 / k_r}{\sqrt{\left[1 - \left(\frac{\omega_{spf}}{\omega_{nr}}\right)^2\right]^2 + \left[2\zeta\left(\frac{\omega_{spf}}{\omega_{nr}}\right)\right]^2}} \tag{3}$$

$F_0$ is the Force on each blade, $k_r$ and $\omega_{nr}$ the stiffness and the natural frequency of each blade and $\zeta$ is the non-dimensional damping. Hence, considering the blade vibration as the displacement $x(t)_r$ for each blade, the pressure distribution around each blade can be mathematically expressed as:

$$P_r = \mathrm{Re}\left\{\sum_{i=0}^{\infty} A_i P e^{ji[\theta + \Omega t + \tilde{\alpha}_r + \gamma_i + B\sin(\omega_{spf}t + \gamma_r)]}\right\} \tag{4}$$

The phase offset of each rotor blade has also been modified in the above expression to account for small deviations in angular location of the rotor blades such that:

$$\tilde{\alpha}_r = [1 + b \times 0.001]\alpha_r$$

where b is a random variable between 0:1.

**Test turbine setup**: A simplified turbine test rig was used to obtain the experimental measurements. The test rig consists of a nineteen (19) flat bladed disk arrangement which is driven by an electric motor. The blades are excited by six (6) high pressure air jets which produce high pressure air streams in the axial direction, which excite the rotor blades as they pass through the high pressure jets.
The test rig is shown in Figure 2, without the external protective housing. Three measurement channels were captured during the run-up and run-down process. The three channels captured were:

Channel 1: Once per rev tachometer signal from a proximity probe located adjacent to the input shaft keyway

Channel 2: Pressure measurement, captured using a flush mounted microphone

Channel 3: Casing vibration measurement, captured using an accelerometer next to the flush mounted microphone

The 19 blades have nominal blade dimensions of 100(L)x50(W)x1.2(T) mm. The mean blade natural frequencies were measured at 117.4 Hz (first bending mode), 515.9 Hz (first torsion mode) and 726 Hz (second bending mode).
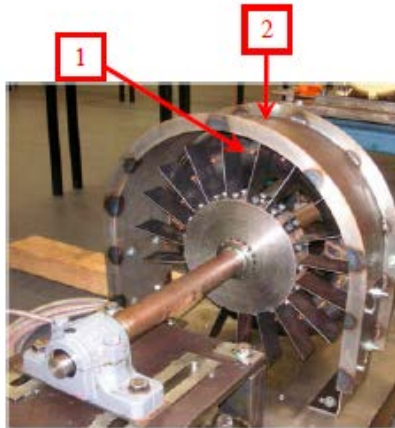
Figure 2. Experimental test rig with 19 blades. (1) 6 air jets located on a toroidal ring which is supplied with high pressure air. (2) location of microphone and accelerometer mounting

After capture, the vibration and pressure measurements were post-processed. This process is outlined in Figure 3, with a 20 second record being captured whilst the test rig was run from 1400–1000 rpm, see Figure 4 for the speed change rate. The measurements were then divided into 32 parts with a nearly constant speed. Each part was order tracked (phase resampled) using the once per-rev tachometer pulse signal. The phase resampled signal was then synchronously averaged to separate the discrete and random portions of the pressure and vibration signals.
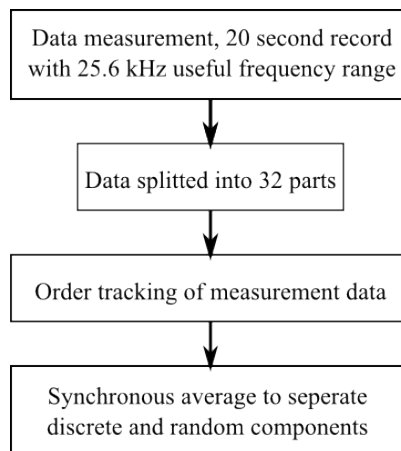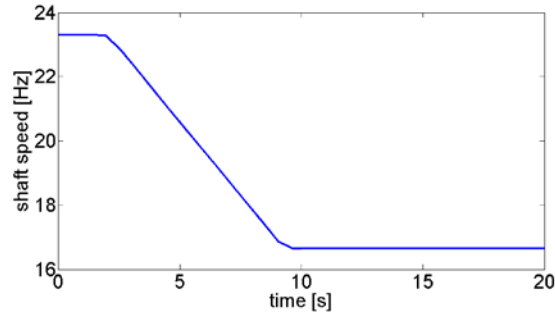


Figure 3. Flow chart of measurement Post-processing

Figure 4. Shaft speed of the turbine test rig as it is run down

**Comparison of internal pressure**: Results were obtained from the measurement data of the turbine test rig and with the aid of an analytical model using the equations of (2), (3) and (4). In the analytical model the force $F_0$ was limited so that B was smaller than $\pi/(2\times19)$. The first two bending mode natural frequencies were included in the analytical model, as the reported natural frequencies were the mean value of all 19 blades, the analytical model included a random variation of up to 2 Hz for each individual blade's natural frequency.
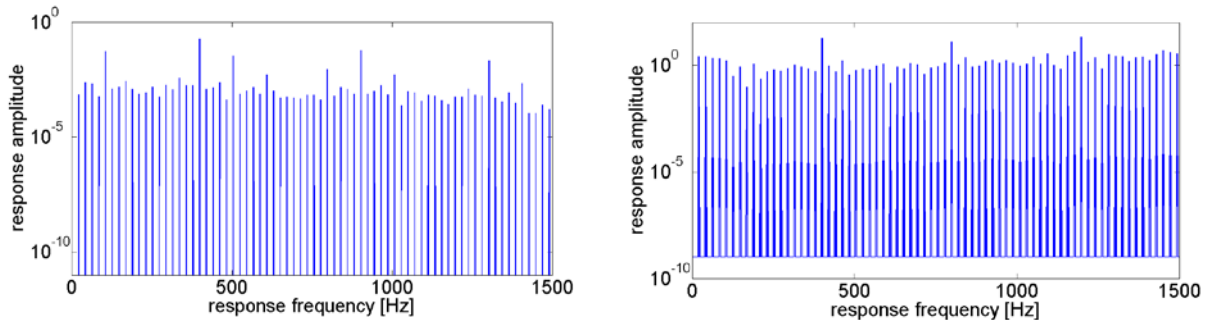


Figure 5. Radial pressure response at shaft speed of 21 Hz, (a) analytical, (b) experimental

Figure 5 shows the separated deterministic radial pressure spectrum at a shaft speed of 21 Hz for the analytical model and for the measurement data. It can be noted that both the analytical deterministic spectrum and the measured pressure spectrum have frequency content at all multiples of shaft speed, with the largest spectral peaks at multiples of blade passing frequency ($19\times\Omega$).
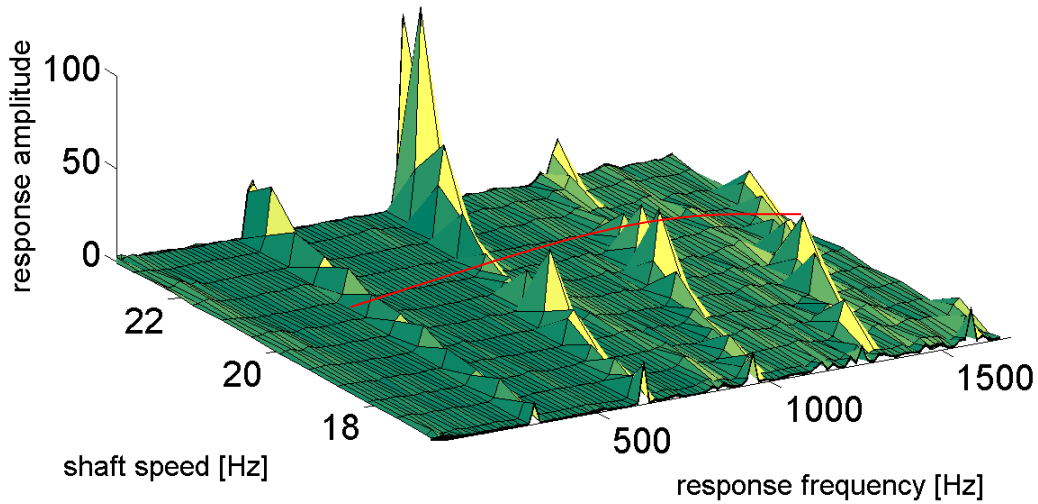
Figure 6. Radial pressure response at shaft speeds from 16.6 – 23.3 Hz, (experimental)

Figure 6 shows the radial pressure response at shaft speeds from 16.6 – 23.3 Hz. The curves with bigger amplitudes represent the first four harmonics at multiples of $\omega_{spf}$. Highlighted by the overlaid line the peaks caused by the increase in phase modulation of the internal pressure signal from the first bending mode can be seen. In Figure 7 these harmonics of shaft speed, except the first, are added together and plotted against shaft speed. The analytical and experimental data show good agreement except of the magnitude, as the magnitude of the pressure in the analytical model is not calibrated from the experimental measurements. The two peaks (marked in red) indicate the frequency of the first and the second bending mode. (remembering the first natural bending mode is approximately 117Hz and with 6 stator blade jets would cause it to be excited at an input shaft speed of 117/6 = 19.5 Hz). The second bending mode is assumed to be excited by the 5th harmonic of $\omega_{bpf}$.
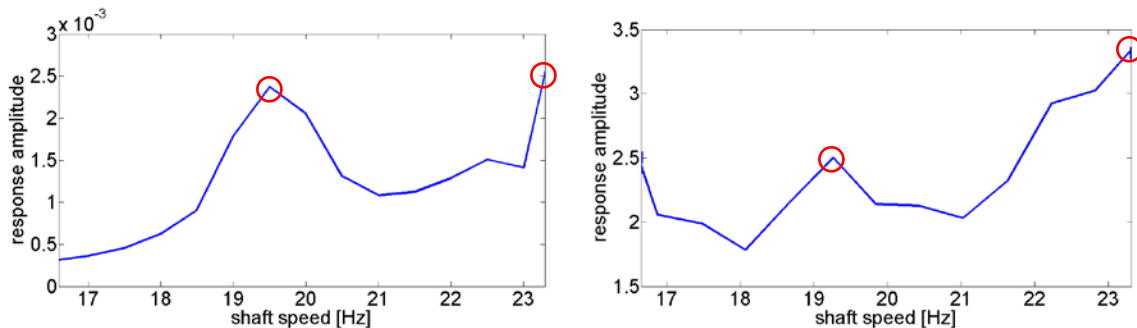


Figure 7. Radial pressure response of the sum of the harmonics at multiples of $\omega_{bpf}$ except of the first harmonic, (a) analytical, (b) experimental

Looking at the single harmonics at multiples of $\omega_{bpf}$ it can be seen that these single harmonics often have a peak in magnitude at each blade natural frequency. The

harmonic, for instance, at $3 \times \omega_{bpf}$ is plotted in Figure 8. It can be seen that both the analytical model of the internal pressure and the experimentally measured internal pressure signal contain a peak around the shaft speed which would excite the first natural frequency.
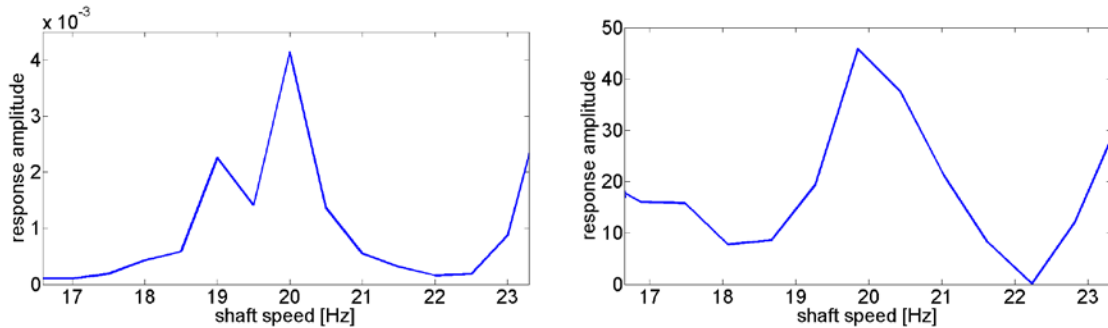


Figure 8. Radial pressure response of the harmonic at $3 \times \omega_{bpf}$ , (a) analytical, (b) experimental

Using the analytical formulation of the internal pressure signal the case of a turbine with a faulty blade was considered. One blade in the analytical model was modified to have one faulty blade given a first bending mode at 69 Hz and the second bending mode at 432 Hz (it should be noted a large difference in natural frequency as shown here would not be seen in practice). Figure 9 demonstrates the effect of the faulty blade. The first and the second bending mode (marked in red) are still present. Additionally there are two new peaks (marked in green) which indicate the natural frequencies of the faulty blade.
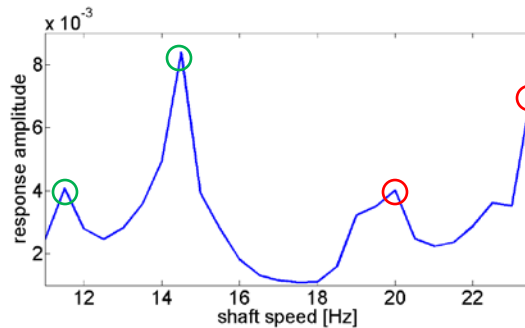


Figure 9. Radial analytical internal pressure spectrum with the sum of the harmonics at multiples of $\omega_{bpf}$ without the first harmonic, (one faulty blade)

**Experimental casing vibration**: The original aim of the work presented here, was to use the external casing vibration to determine the properties of the vibration of the rotor blades. The development of the analytical internal pressure signal for a turbine with rotor blade vibration was developed and shown to contain information about the rotor blade vibration in the previous section. Due to the driving pressure force containing blade vibration, the casing vibration should also contain rotor blade vibration information. It has been shown that the transfer of the internal pressure signal to casing vibration will be of the same form, and the casing transfer will simply act as a linear time invariant filter [5]. Figure 10 shows the deterministic component of the radial casing vibration spectrum

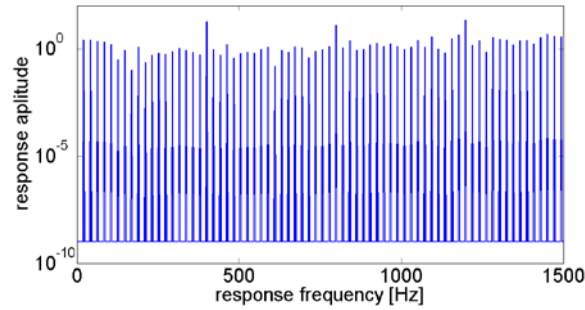at shaft speed of 21 Hz, which can be seen to be qualitatively similar to the internal pressure spectrum.



Figure 10. Radial casing deterministic vibration spectrum at shaft speed of 21 Hz, (experimental)

Figure 11 (a) shows the radial casing response of the sum of the harmonics at multiples of $\omega_{bpf}$ excluding the first blade passing frequency harmonic. In comparison with Figure 7 (b) the peak at the first natural frequency is not very noticeable. However when some of the individual harmonics of blade pass frequency are observed individually the harmonics do show a sharp peak at the first bending mode frequency, similar to the internal pressure signal. For example in Figure 11(b) the third harmonic of blade pass frequency is shown for the changing input shaft speed. This can be compared to Figure 8(b) where a similar peak is shown in the internal pressure signal.
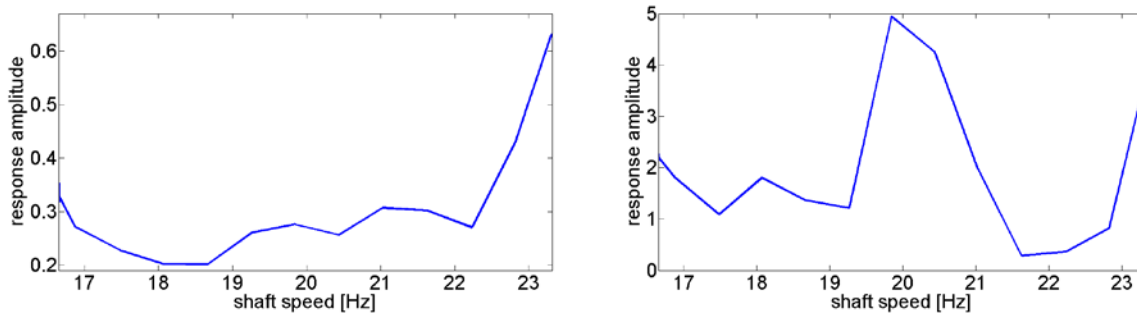


Figure 11. Radial casing response, (a) of the sum of the harmonics at multiples of $\omega_{bpf}$ except first harmonic, (b) harmonic at $3 \times \omega_{bpf}$

**Conclusions:**

External casing vibration measurements, and the internal pressure signal measured on a simplified turbine test rig were shown to contain information about rotor blade vibration within the presented results. This simplified turbine was swept over a range of running speeds which would excite the first bending mode of the rotor blades. During the sweeping of the engine over this speed range, a peak in both the internal pressure and casing vibration spectrum could be seen. This would then allow estimation of the rotor blade natural frequencies. An analytical model of the internal pressure signal in a turbine with blade vibration was also presented. The results from the experimental setup and the analytical model produced qualitatively similar results. An additional result for a

simulated faulty rotor blade was shown using the analytical internal pressure signal model. The results given showed that a reduction in the blade natural frequency was also able to be identified from the analytical model of the pressure spectrum.

**References**:

1.      Lawson, C.P. and P.C. Ivey, *Turbomachinery blade vibration amplitude measurement through tip timing with capacitance tip clearance probes.* Sensors and Actuators A (Physical), 2005. **118**(1): p. 14-24.
2.      Heath, S. and M. Imregun, *Improved single-parameter tip-timing method for turbomachinery blade vibration measurements using optical laser probes.* International Journal of Mechanical Sciences, 1996. **38**(10): p. 1047-1058.
3.      Forbes, G.L. and R.B. Randall. *Simulated Gas Turbine Casing Response to Rotor Blade Pressure Excitation*. in *5th Australasian Congress on Applied Mechanics*. 2007. Brisbane, Australia.
4.      Forbes, G.L. and R.B. Randall, *Estimation of turbine blade natural frequencies from casing pressure and vibration measurements.* Mechanical Systems and Signal Processing, 2013. **36**(2): p. 549-561.
5.      Forbes, G.L., *Non-contact gas turbine blade vibration monitoring using internal pressure and casing response measurements*, 2010, The University of New South Wales: PhD Dissertation. p. 211.